IEEE Photonics Journal
An IEEE Photonics Society Publication

Open Access

Supercontinuum Generation by Using a Highly Germania-Doped Fiber With a High-Power Proportion Beyond 2400 nm

Volume 11, Number 6, December 2019

Zhijian Zheng
Deqin Ouyang
Jinzhang Wang
Chunyu Guo
Jihong Pei
Shuangchen Ruan

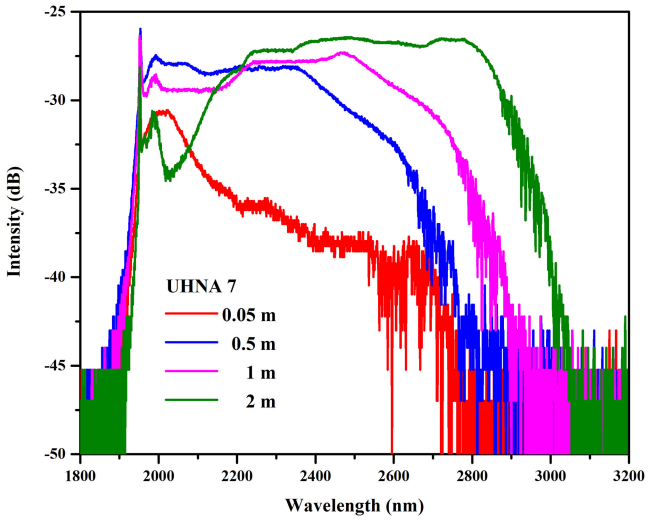

DOI: 10.1109/JPHOT.2019.2953215

IEEE photonics SOCIETY
IEEE

Supercontinuum Generation by Using a Highly Germania-Doped Fiber With a High-Power Proportion Beyond 2400 nm

Zhijian Zheng,[1,2] **Deqin Ouyang**,[3] **Jinzhang Wang**,[1] **Chunyu Guo**,[1] **Jihong Pei**,[4] **and Shuangchen Ruan** [1,2]

[1]Shenzhen Key Laboratory of Laser Engineering, Key Laboratory of Advanced Optical Precision Manufacturing Technology of Guangdong Higher Education Institutes, Guangdong Provincial Key Laboratory of Micro/Nano Optomechatronics Engineering, College of Physics and Optoelectronic Engineering, Shenzhen University, Shenzhen 518060, China
[2]College of New Materials and New Energies, Shenzhen Technology University, Shenzhen 518118, China
[3]Sino-German College of Intelligent Manufacturing, Shenzhen Technology University, Shenzhen 518118, China
[4]Key Laboratory of ATR National Defense Science and Technology, College of Electronics and Information Engineering, Shenzhen University, Shenzhen 518060, China

DOI:10.1109/JPHOT.2019.2953215

Manuscript received September 17, 2019; revised October 19, 2019; accepted November 9, 2019. Date of publication November 12, 2019; date of current version December 17, 2019. This work was supported in part by the National Natural Science Foundation of China under Grants 61905151, 61575129, and 61605122; in part by the Guangdong Natural Science Foundation under Grant 2016A030310049; in part by the Major Science and Technology Project of Guangdong Province under Grant 2014B010131006; and in part by the Shenzhen Science and Technology under Projects KQJSCX20160226194031 and JCYJ20160520161351540. Corresponding author: Shuangchen Ruan (e-mail: scruan@sztu.edu.cn).

Abstract: A high-power all-fiber supercontinuum (SC) source in a highly germania-doped fiber (GDF) pumped by a picosecond thulium-doped master oscillator power amplifier (MOPA) system is presented. By further optimizing the length of the GDF, the long-wavelength edge of the wideband flat SC can be broadened to 3 μm. The flat SC has an average output power of 11.62 W and a 3 dB bandwidth of 750 nm. The power proportion beyond 2400 nm is as high as 55.3%. To our knowledge, this SC average output power is the highest from a highly GDF.

Index Terms: Thulium-doped fiber lasers, supercontinuum generation, pulsed lasers, laser amplifiers, fiber optics.

1. Introduction

The supercontinuum (SC) source has attracted widespread attention owing to its superior characteristics such as high brightness, high spatial coherence, broad bandwidth, and good beam quality [1]–[3]. Such features are useful for biophotonics [4], [5], light detection and ranging system [6], [7], chemical sensing [8], [9], and metrology [10], [11]. Germania fibers [12]–[18] and soft glass fibers [19]–[24] are extensively applied in supercontinuum generation (SCG). Germania fibers are easy to handle and compatible with fiber laser systems consisting of silica pigtails and are suitable for SCG covering the near-IR. Mid-IR SC is difficult to achieve using germania fibers because of their high mid-IR transmission loss. Soft glass fibers exhibit lower phonon energy and lower mid-IR transmission loss than germania fibers, making the former more suitable for

Fig. 1. Experimental setup of the SC source.

propagating SC at mid-IR region. Although soft glass fibers are regarded as an excellent candidate for mid-IR SCG, their shortcomings are evident. Soft glass fibers are subject to moisture, their low transition temperature makes them too hard to splice with silica fibers, and they have low mechanical resistance. Considering these drawbacks, germania fibers have important application value in SCG at near-IR to mid-IR regions.

In recent years, different kinds of germania fibers, such as highly germania-doped fiber (GDF) and pure germania-core fiber (GCF), have been widely used to generate SC at 2–3 μm region. In 2012, Kamynin *et al.* first reported a SC source with spectrum broadened to 2.7 μm based on a segment of highly GDF (64 mol.%) and a nanosecond erbium-doped fiber laser [12]. The output power was 0.49 W, and the power distribution in the range of 2–2.6 μm was 55%. Later, Zhang *et al.* demonstrated a SC source based on a highly GDF (75 mol.%) with an optimized spectrum ranging from 1.9 to 3 μm [13]. However, a free-space compressor was introduced into the system, which would reduce the stability and increase the complexity. In 2014, Anashkina *et al.* constructed an all-fiber femtosecond laser system for pumping a piece of ultra-highly GDF (97 mol.%) [14]. A milliwatt-level SC source was realized with a corresponding spectrum range of 1.9–3 μm. Anashkina also theoretically demonstrated that the spectrum edge can be broadened to 3.5 μm with optimal fiber parameters. Subsequently, Yin *et al.* experimentally demonstrated a 6.12 W all-fiber SC laser source whose spectrum spanned to 3.6 μm in a 12-cm-long pure GCF [15]. Later on, Yin boosted the output power to 30.1 W utilizing a longer pure GCF with a larger core diameter, and the obtained 10 dB spectral bandwidth ranged from 1.95 to 3.0 μm [16]. The larger core diameter reduces the bandwidth gain versus pump power efficiency. Although GCFs exhibit excellent features, they are not widely commercialized and are much more expensive than GDFs. Studying the low-cost high-power GDF-based SC source remains of great research significance. In 2016, Jain *et al.* realized an ultra-broadband mid-IR SC source with a segment of GDF (74 mol.%) by using a four-stage erbium-doped fiber amplifier [17]. The obtained widest spectrum range was 0.7 to 3.2 μm and the power is 1.44 W. The corresponding spectrum was only broadened to 2.7 μm at the highest output power of 6.4 W. Recently, Jain *et al.* have further scaled the power of a 2–3 μm GDF-based SC source to 6 W, but the flatness of the spectrum was poor [25].

In this work, we report an all-fiber high-power GDF-based SC source with a high mid-IR power proportion. At the maximum output power of 18.13 W, a SC with spectrum ranging from 1.9 to 2.7 μm is achieved. By optimizing the length of the GDF, spectrum can be extended to 3.05 μm. Output power is decreased to 11.62 W, and power proportion beyond 2400 nm is increased to 55.3%. To our knowledge, this is the highest 2–3 μm SC output power from a highly GDF.

2. Experimental Setup and Results

2.1 Experimental Setup

The experimental setup of the SC source is presented in Fig. 1. The SC source contains a master oscillator power amplifier (MOPA) system and a segment of nonlinear optical fiber. The master oscillator is a home-made SESAM-based picosecond thulium-doped fiber laser (TDFL). The cavity of the TDFL is linear, and it includes an SESAM and a fiber Bragg grating. The single-mode 1550 nm pump light is injected into the thulium-doped fiber via a wavelength division multiplexer. The thulium-doped fiber is SM-TSF-5/125 that is 9-cm-long. The core NA is 0.24, and the core absorption coefficient is 340 dB/m at 1560 nm. The total linear cavity length is approximately

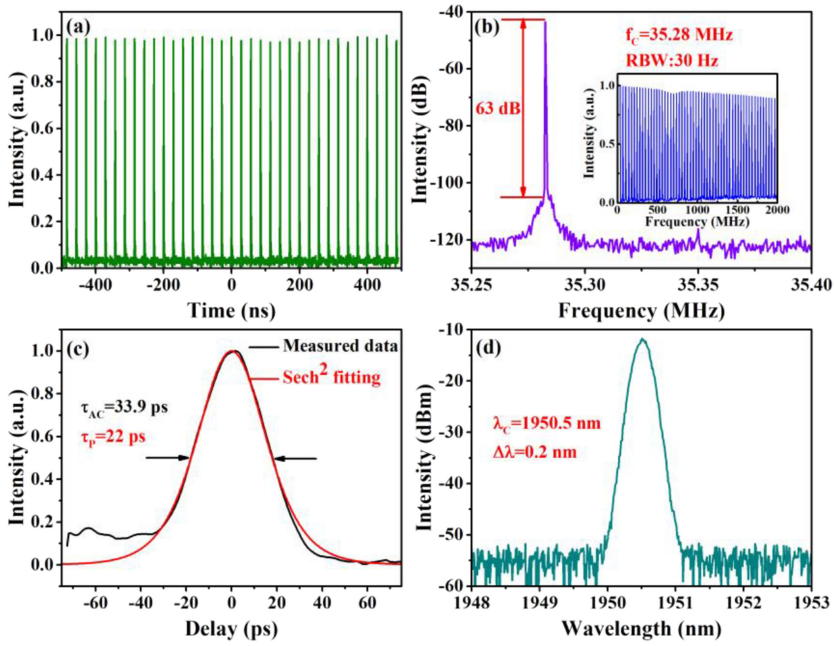

Fig. 2. (a) Pulse train; (b) RF spectrum. Inset: RF spectrum with 2 GHz spans (resolution bandwidth: 10 kHz); (c) Autocorrelation trace; (d) Optical spectrum.

2.8 m. A pigtailed ISO is utilized to connect the master oscillator and the pre-amplifier, and doing so ensures the unidirectional transmission and prevents parasitic lasing. Similarly, an ISO is added between the amplifiers. The pre-amplifier is a thulium-doped fiber amplifier (TDFA), which has a thulium-doped double-cladding gain fiber and a 793 nm laser (LD). The thulium-doped fiber is SM-TDF-10P/130-HE that is 3-m-long. The core NA is 0.15, and the cladding absorption coefficient is 3 dB/m at 793 nm. After the pre-amplifier, a large-mode-area TDFA (LMA-TDFA) is used to further boost the output power. The LMA-TDFA contains a segment of LMA-TDF (Nufern, LMA-TDF-25P/250-HE) and a 793 nm LD. The LMA-TDF has a core NA of 0.09 and a high cladding absorption coefficient of 9.5 dB/m at 793 nm. The high-power 793 nm LD is employed to pump the LMA-TDF. A mode-field adapter (MFA) is used for mode-field matching between the two amplifiers. Similarly, a high-power backward MFA is utilized to link the MOPA system and the nonlinear optical fiber. The pigtails of the backward MFA are precision-matched passive LMA double-cladding fiber (Nufern, LMA-GDF-25/250-M) and single-mode fiber (Nufern, SM1950), respectively. A piece of silica-based highly GDF (Nufern, UHNA 7) serves as the nonlinear optical fiber, which is directly spliced to the SM1950 fiber.

2.2 Properties of the Mode-Locked Master Oscillator

The characteristics of the mode-locked master oscillator are shown in Fig. 2. Fig. 2(a) plots the output pulse train at the fundamental repetition rate, which is measured using a 2 μm-band photodetector (ET-5000), connected with a Tektronix digital oscilloscope (DPO 7104C). The fundamental repetition rate corresponds to the oscillator cavity length. The radio frequency (RF) spectrum of the master oscillator is presented in Fig. 2. The resolution bandwidth (RBW) for the RF spectrum is 30 Hz. The measured RF spectrum is centered at 35.28 MHz with a corresponding signal-to-noise ratio (SNR) is 63 dB. The RF spectrum in the 2 GHz span using a 10 kHz RBW is illustrated in the inset of Fig. 2(b). The pulse train and RF spectra confirm that the oscillator is operating in a steady state. The autocorrelation (AC) trace of the output pulses is measured using

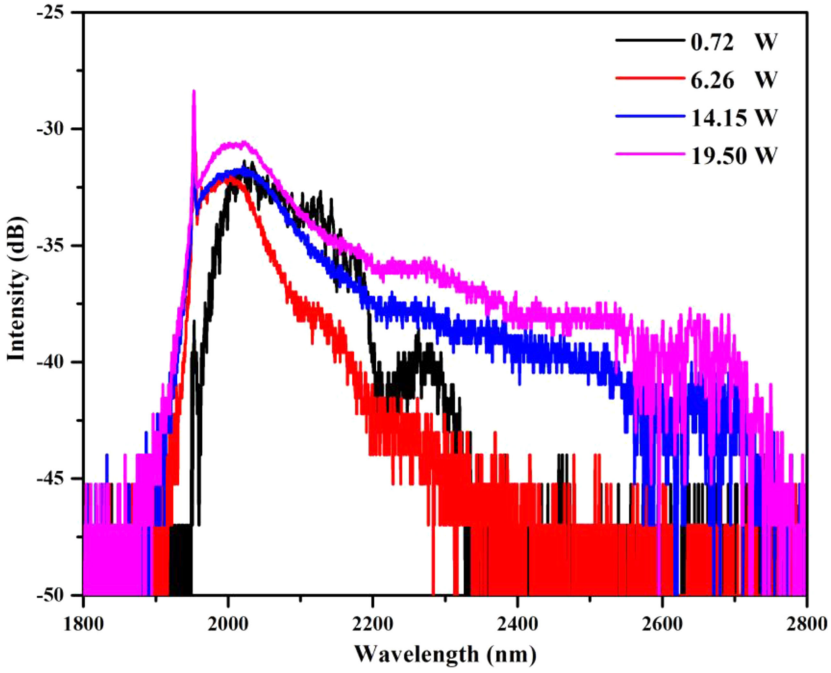

Fig. 3. Evolution of the output spectra of the SM1950 fiber at different output powers.

an autocorrelator (APE, pulseCheck USB). Fig. 2(c) depicts the measured AC trace, and the FWHM is 33.9 ps. With a sech^2-fitting, the pulse width is 22 ps. A positive base is on the left side of the AC trace, which can also be found in Ref. [18]. We think the positive base is mainly because of the autocorrelator's low sensitivity. The optical spectrum is measured by a long-wavelength spectrum analyzer (YOKOGAWA, AQ6375B) and plots in Fig. 2(d). The resolution for the optical spectrum is 0.05 nm. The measured spectrum is centered at 1950.5 nm with a 3 dB bandwidth of 0.2 nm.

2.3 Properties of the Supercontinuum Generation

The pulses are further amplified in a two-stage MOPA system. With the help of a high-power backward MFA, the amplified pulses are then injected into the nonlinear optical fiber. The interaction of dispersion and nonlinear processes (e.g., self-phase modulation (SPM), four-wave mixing, and soliton based dynamics) will lead to spectral broadening [3]. In our experiment, the SCG is measured using a high-performing FTIR spectrometer (Bruker, Tensor 27). Fig. 3 shows the evolution of the output spectra of the SM1950 fiber at different output powers. When the LMA-TDFA has no 793 nm pump power, the LMA-TDFA has an output power of 0.72 W and the spectrum is broadened to 2.33 μm. As the pump power increases, the output power increases and the spectrum broadens. When the output power is increased to 19.50 W, the SC is extended to 2.7 μm, and the corresponding 3 dB bandwidth is 150 nm. As in Ref. [3], the attenuation curve of silica-based fiber exhibits an exponential increase when wavelength is beyond 2000 nm. Therefore, the obtained long-wavelength edge is located in the ultra-high loss area of the silica-based fiber.

To further extend the output spectra, a segment of ultra-high NA single-mode GDF (UHNA 7) is spliced to the SM1950 fiber. The MOPA system with SM1950 pigtail is used as the pump source for the UHNA 7 fiber. The UHNA 7 fiber has a core/cladding diameter of 2.4/125 μm, a core NA of 0.41, a zero-dispersion wavelength of 2.6 μm, and a high germania doping concentration of 30 mol.% [26], [27]. The SM1950 fiber is a single-mode 2 μm beam delivery fiber. The core/cladding diameter, core NA, and single-mode cutoff wavelength are 7/125 μm, 0.2, and 1750 nm, respectively. Despite

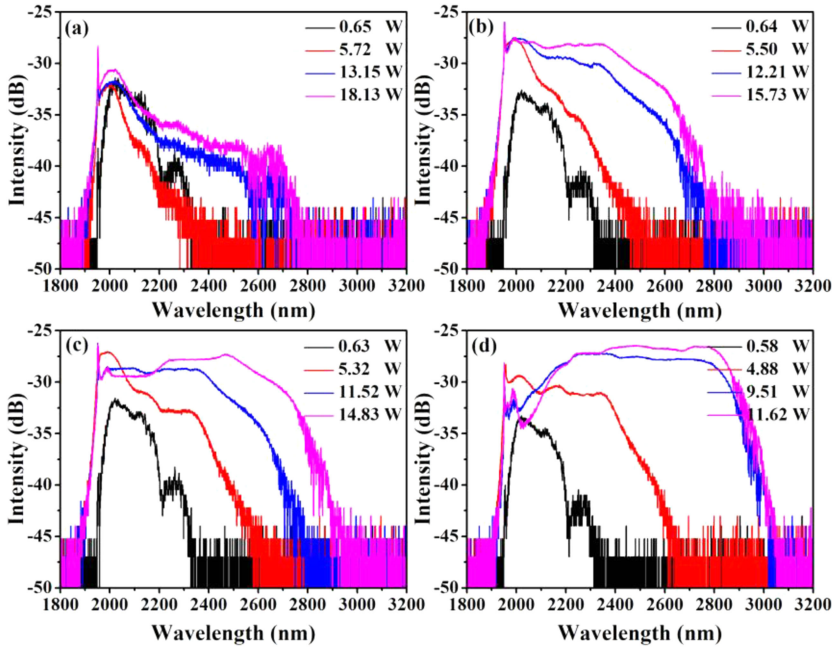

Fig. 4. Evolution of the output spectra from (a) 0.05 m, (b) 0.5 m, (c) 1 m, and (d) 2 m UHNA 7 fiber at different output powers.

the large mode-field mismatch of these two fibers, the splice loss can be reduced by repeating the arc discharge on the splice junction using a commercial fusion splicer. Under the effect of repeated arc discharge, the fiber core of the UHNA 7 is gradually expanding, and optimized MFD match can be achieved. Finally, a splice loss of 0.3 dB is obtained at the low-power regime.

Fig. 4 shows the evolution of output spectra from different lengths of UHNA 7 fiber. The output spectra measured from a 0.05-m-long UHNA 7 fiber are shown in Fig. 4(a), which is similar to the direct output of the SM1950 fiber. The maximum output power is decreased to 18.13 W mainly due to the splice loss of the fibers. Figs. 4(b)–(d) show an increase in spectrum broadening when the length of UHNA 7 fiber is lengthened to 0.5, 1, and 2 m. At the maximum output power, the corresponding 3 dB bandwidth is extended to 550, 740, and 750 nm, respectively. As the length of the UHNA 7 fiber is further increased, the output power is further reduced, although the output spectrum is not further broadened. In our experiment, 2 m is the optimal length of the UHNA 7 fiber. When the wavelength is $>$2400 nm, the loss of the UHNA 7 fiber exponentially increases with respect to the operating wavelength. As Ref. [26] shows, the loss at 2400 nm is 0.7 dB/m and it dramatically increases up to 4.5 dB/m at 2500 nm. Longer UHNA 7 fiber not only introduces higher nonlinearity but also introduces higher fiber attenuation at the long-wavelength region.

The output spectra of the UHNA 7 fiber with different lengths at the maximum output power are plotted in Fig. 5. Spectral intensity beyond 2400 nm demonstrates an apparent increase with respect to the length of the UHNA 7 fiber. When the UHNA 7 fiber is 2-m-long, the output spectrum has the widest range, that is, from 1.92 to 3.05 μm. The SC power distribution beyond 2400 nm is also calculated using spectral integration. For SM1950 fiber, the power proportion beyond 2400 nm is 41.8% at the maximum output power, which is nearly twice as large as that reported in Ref. [28]. The power proportion beyond 2400 nm is further optimized by the UHNA 7 fiber. As the length of the UHNA 7 fiber increases, the power proportion beyond 2400 nm increases to 41.8%, 52.32%, 54.9%, and 55.3%. The UHNA 7 fiber is pumped in the normal and anomalous dispersion regimes. However, the pump energy in the anomalous dispersion regime is weak, and most of the energy is located in the normal dispersion regime. Therefore, at the beginning, the main nonlinear effect that

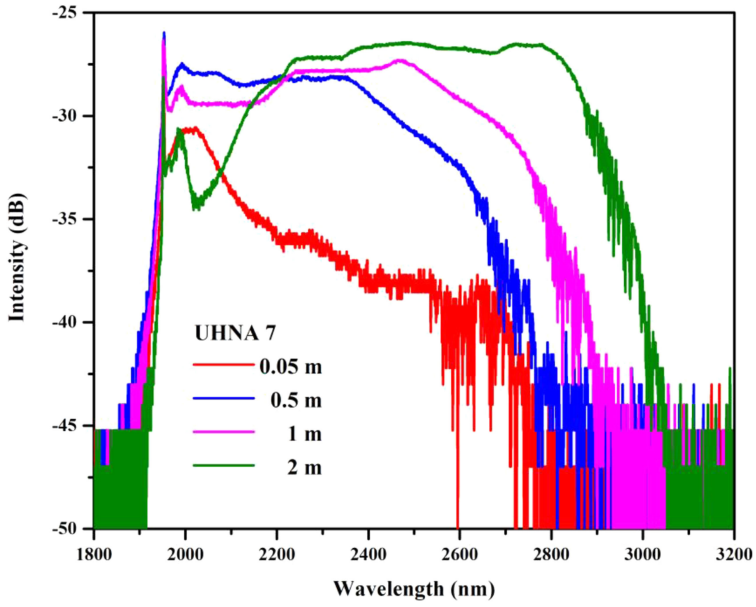

Fig. 5. Supercontinuum generated from UHNA 7 fiber at different lengths at maximum output power.

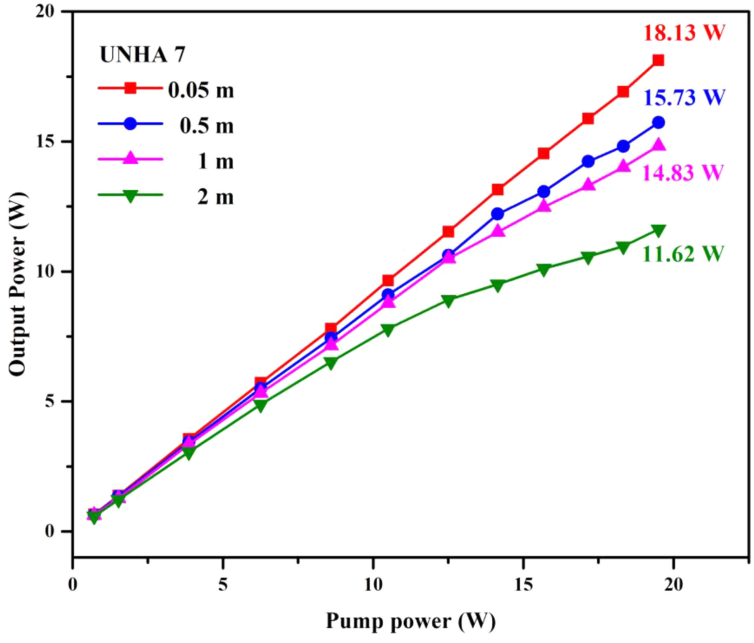

Fig. 6. Output power of the UHNA 7 fibers versus the pump power.

leads to spectral broadening should be stimulated Raman scattering (SRS), and the SCG depends on the interaction among SRS, cross-phase modulation, and SPM [3].

Fig. 6 depicts the relationship between the output power of the UHNA 7 fibers versus the pump power. The maximum output power is obtained from the 0.05-m-long UHNA 7 fiber, which is 18.13 W. The output power increases linearly with pump power with a slope efficiency of 92%. The UHNA 7 fiber used here has a short length, so the output spectrum is almost the same as that of the SM1950. When the length of the UHNA 7 fiber is extended to 0.5-m-long, the output power is reduced to 15.73 W. In addition, the slope efficiency is reduced to 81%, and the spectrum

is broadened to 2.8 μm. As the length of the UHNA 7 fiber is further extended, the output power and slope efficiency are drastically reduced due to high fiber attenuation and spectral broadening. Longer nonlinear fibers not only reduce the output of the SC but also result in a flatter and wider spectrum (see Fig. 5). When the length of the UHNA 7 fiber is lengthened to 2-m-long, the flattest SC is obtained. When the output power is 11.62 W, the spectrum covers from 1.92 to 3.05 μm with a 3 dB bandwidth of 750 nm and a power proportion beyond 2400 nm of 55.3%.

3. Conclusions

We demonstrate a spectrum-optimized high-power GDF-based SC source. By optimizing the length of the GDF, a SC output with an average power of 11.62 W and a spectrum range of 1.92–3.05 μm is obtained. The power proportion beyond 2400 nm is as high as 55.3%. This SC average output power is the highest based on a highly GDF nonlinear fiber. This SC source will be beneficial for pumping soft glass fibers or chalcogenide bulk glass to broaden the spectrum to 5 μm. In future work, we will concentrate on high mid-IR power proportion SC source.

References

[1] I. Sorokina, V. Dvoyrin, N. Tolstik, and E. Sorokin, "Mid-IR ultrashort pulsed fiber-based lasers," *IEEE J. Sel. Topics Quantum Electron.*, vol. 20, no. 5, pp. 99–110, Sep./Oct. 2014.

[2] J. Dudley, G. Genty, and S. Coen, "Supercontinuum generation in photonic crystal fiber," *Rev. Modern Phys.*, vol. 78, no. 4, pp. 1135–1184, 2006.

[3] J. Swiderski, "High power mid-infrared supercontinuum sources: Current status and future perspectives," *Prog. Quantum Electron.*, vol. 38, no. 5, pp. 189–235, 2014.

[4] H. Tu and S. Boppart, "Coherent fiber supercontinuum for biophotonics," *Laser Photon. Rev.*, vol. 7, no. 5, pp. 628–645, 2013.

[5] J. Taylor and J. Biomed, "Tutorial on fiber-based sources for biophotonic applications," *J. Biomed. Opt.*, vol. 21, no. 6, 2016, Art. no. 061010.

[6] G. Méjean *et al.*, "Towards a supercontinuum-based infrared lidar," *Appl. Phys. B*, vol. 77, no. 2, pp. 357–359, 2003.

[7] Y. Chen *et al.*, "Two-channel hyperspectral LiDAR with a supercontinuum laser source," *Sensors*, vol. 10, no. 7, pp. 7057–7066, 2010.

[8] C. Kaminski, R. Watt, A. Elder, J. Frank, and J. Hult, "Supercontinuum radiation for applications in chemical sensing and microscopy," *Appl. Phys. B*, vol. 92, no. 3, pp. 367–378, 2008.

[9] A. Cubillas *et al.*, "Photonic crystal fibres for chemical sensing and photochemistry," *Chem. Soc. Rev.*, vol. 42, no. 22, pp. 8629–8648, 2013.

[10] J. Woodward *et al.*, "Supercontinuum sources for metrology," *Metrologia*, vol. 46, no. 4, pp. S277–S282, 2009.

[11] N. Nishizawa, "Wideband ultrafast fiber laser sources for OCT and metrology," *J. Phys. B: At. Mol. Opt. Phys.*, vol. 49, no. 18, 2016, Art. no. 182003.

[12] V. Kamyni, A. Kurkov, and V. Mashinsky, "Supercontinuum generation up to 2.7 μm in the germanate-glass-core and silica-glass-cladding fiber," *Laser Phys. Lett.*, vol. 9, no. 3, pp. 219–222, 2012.

[13] M. Zhang *et al.*, "Mid-infrared Raman-soliton continuum pumped by a nanotube-mode-locked sub-picosecond Tm-doped MOPFA," *Opt. Express*, vol. 21, no. 20, pp. 23261–23271, 2013.

[14] E. Anashkina, A. Andrianov, M. Koptev, S. Muravyev, and A. Kim, "Towards mid-infrared supercontinuum generation with germano-silicate fibers," *IEEE J. Sel. Topics Quantum Electron.*, vol. 20, no. 5, pp. 643–650, Sep./Oct. 2014.

[15] K. Yin, B. Zhang, J. Yao, L. Yang, G. Liu, and J. Hou, "1.9-3.6 μm supercontinuum generation in a very short highly nonlinear germania fiber with a high mid-infrared power ratio," *Opt. Lett.*, vol. 41, no. 21, pp. 5067–5070, 2016.

[16] K. Yin, B. Zhang, L. Yang, and J. Hou, "30 W monolithic 2–3 μm supercontinuum laser," *Photon. Res.*, vol. 6, no. 2, pp. 123–126, 2018.

[17] D. Jain, R. Sidharthan, P. Moselund, S. Yoo, D. Ho, and O. Bang, "Record power, ultra-broadband supercontinuum source based on highly GeO_2 doped silica fiber," *Opt. Express*, vol. 24, no. 23, pp. 26667–26677, 2016.

[18] Z. Zheng *et al.*, "Dual-operation regime thulium-doped fiber laser and its applications in cascaded Raman light and supercontinuum generation," *IEEE Photon. J.*, vol. 10, no. 1, Feb. 2018, Art. no. 1500809.

[19] K. Liu, J. Liu, H. Shi, F. Tan, and P. Wang, "High power mid-infrared supercontinuum generation in a single-mode ZBLAN fiber with up to 21.8 W average output power," *Opt. Express*, vol. 22, no. 20, pp. 24384–24391, 2014.

[20] Z. Zheng *et al.*, "Scaling all-fiber mid-infrared supercontinuum up to 10 W-level based on thermal-spliced silica fiber and ZBLAN fiber," *Photon. Res.*, vol. 4, no. 4, pp. 135–139, 2016.

[21] Z. Zhao *et al.*, "Mid-infrared supercontinuum covering 2.0–16 μm in a low-loss telluride single-mode fiber," *Laser Photon. Rev.*, vol. 11, no. 2, 2017, Art. no. 1700005.

[22] S. Kedenburg *et al.*, "High repetition rate mid-infrared supercontinuum generation from 1.3 to 5.3 μm in robust step-index tellurite fibers," *J. Opt. Soc. Amer. B*, vol. 34, no. 3, pp. 601–607, 2017.

[23] T. Cheng *et al.*, "Mid-infrared supercontinuum generation spanning 2.0 to 15.1 μm in a chalcogenide step-index fiber," *Opt. Lett.*, vol. 41, no. 9, pp. 2117–2120, 2016.

[24] R. Thapa *et al.*, "Low-loss, robust fusion splicing of silica to chalcogenide fiber for integrated mid-infrared laser technology development," *Opt. Lett.*, vol. 40, no. 21, pp. 5074–5077, 2015.
[25] D. Jain *et al.*, "Scaling power, bandwidth, and efficiency of mid-infrared supercontinuum source based on a GeO_2-doped silica fiber," *J. Opt. Soc. Amer. B*, vol. 36, no. 2, pp. 86–92, 2019.
[26] H. Jiang, L. Zhang, and Y. Feng, "Silica-based fiber Raman laser at $>$2.4 μm," *Opt. Lett.*, vol. 40, no. 14, pp. 3249–3252, 2015.
[27] K. Kieu, L. Schneebeli, J. Hales, J. Perry, R. Norwood, and N. Peyghambarian, "Demonstration of Zeno switching through inverse Raman scattering in an optical fiber," *Opt. Express*, vol. 19, no. 13, pp. 12532–12539, 2011.
[28] J. Swiderski and M. Michalska, "Mid-infrared supercontinuum generation in a single-mode thulium-doped fiber amplifier," *Laser Phys. Lett.*, vol. 10, 2013, Art. no. 0351053.